CrystEngComm

Accepted Manuscript

ROYAL SOCIETY OF CHEMISTRY

www.rsc.org/crystengcomm

Cite this: DOI: 10.1039/x0xx00000x

Halogen–halogen interaction and halogen bonding in thiacalixarene systems

Manabu Yamada*[a], Ryo Kanazawa[b], and Fumio Hamada*[c]

Received 00th January 2012,
Accepted 00th January 2012

DOI: 10.1039/x0xx00000x

www.rsc.org/

Crystals of 5,11,17,23-tetraiodo-25,26,27,28-tetrapropoxy thiacalix[4]arene (**2**) exhibited I···I halogen–halogen interaction between each of the thiacalixarene molecules, ca. 2% shorter than the respective van der Waals atomic radii. Further support for S–π and C–H···I interactions and hydrogen bonding was provided by the formation and characterization of a three-dimensional supramolecular assembly of **2** via preferential intermolecular I···I interactions. In contrast, crystals of 5,11,17,23-tetraiodo-25,26,27,28-tetrabutoxy thiacalix[4]arene (**3**) were identified to have S···I halogen bonding ca. 4.5% shorter than the respective van der Waals atomic radii. The extended structure of **3** also formed a three-dimensional supramolecular assembly exhibiting S···I halogen bonding and hydrogen bonding, in addition to ancillary S–π and C–H···I interactions. We have also elucidated I···I and S···I interactions by computational approaches.

Introduction

The past decade has seen continued intensive investigations of the so-called non-covalent interactions (i.e., hydrogen bonding, electrostatic, and van der Waals interactions), owing to their intriguing properties for use in molecular recognition applications, complex biological systems, and construction of fascinating supramolecular assemblies.[1] The weak non-covalent intermolecular interactions of halogen atoms such as halogen bonding[2] and halogen–halogen interactions[3] have also attracted significant recent attention for their key roles in regulating molecular assemblies. Although both interactions are governed by a high tendency to occur along the extended C–X (X = halogen atoms) axis, these forces are being increasingly used to facilitate formation of supramolecular assemblies and mediate molecular recognition events, thus providing a useful tool for crystal formation or molecular recognition in the field of crystal engineering and solution chemistry. Supramolecular assemblies involving specific interactions between host molecules and/or guest molecules have been shown to express a variety of supramolecular functionalities, since the strengths of non-covalent interactions make it possible to control the aggregation of molecular building blocks in the solid, liquid, and gas phases. Furthermore, non-covalent intra- and intermolecular forces play an important role in the formation of supramolecular assemblies and triggering of biomolecular activities via molecular recognition events occurring in supramolecular and living systems.[4]

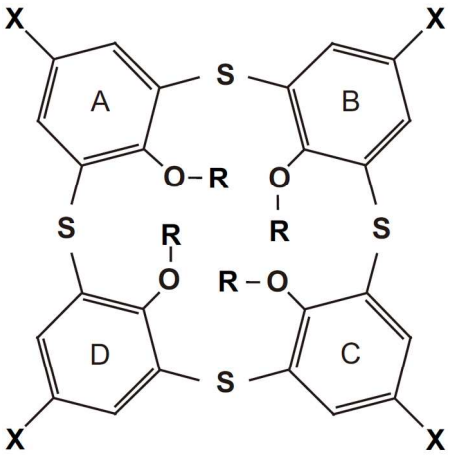

1; X = Br, R = Butyl
2; X = I, R = Propyl
3; X = I, R = Butyl

Scheme 1 Structural formulas of thiacalix[4]arene derivatives **1**–**3**.

Halogen bonding is described as a weak, short-range interaction, similar to that found in the more well-known hydrogen bonding interaction, occurring between polarizable halogen atoms X as electrophilic species (electron acceptors) and heteroatoms D (D = O, N, S, P, etc.) as lone pair–possessing species (electron donors) in Lewis acid–base pairs.[2] The C–X···D angles are defined as 140–180º and the X···D distances are shorter than sum of the van der Waals radii of the X and D atoms. In contrast, halogen–halogen interactions have been broadly defined as arising from the polarization and dispersion–repulsion interactions of halogen atoms in the crystalline state. Two types of halogen–halogen interactions exist; namely Type I and Type II. A C–X···X–C contact is considered a true halogen–halogen interaction when their interhalogen distances are less than the sum of their van der Waals radii because of an attractive $X^{\delta+}\cdots X^{\delta-}$ interaction.[3] The distinction between the two types of halogen-halogen interaction is based on the two angles centered on the halogen atoms; the angles are defined as $\theta_1 = \theta_2 = 140–180º$ for Type I, and $\theta_1 = 150–180º$, $\theta_2 = 90–120º$ for Type II (ESI; Fig. S1).

Resnati and co-workers have reported extensively on the interactions involving solid-state halogen bonding in diverse substances such as biomolecules, halogenated alkanes, halogenated phenols, and host molecule–polymer combinations from a crystallographic perspective.[5] They have also described

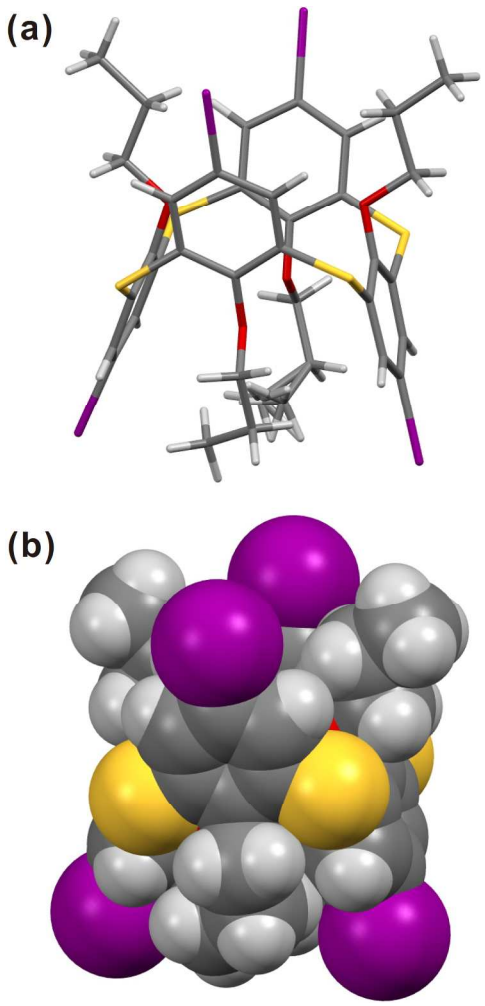

Fig. 1 (a) Stick diagram and (b) space-filling representation of the molecular structure of **2**. I = purple, S = yellow, O = red, C = dark grey, H = light gray.

the efficient construction of three-dimensional supramolecular architectures via halogen bonding as a directing force in the crystalline state, demonstrating this phenomenon using haloperfluoroalkane or halotetrafluorophenol derivatives as strong acceptors in combination with basic amine and imine nitrogen donors. Similarly, we have revealed the possibility of intermolecular interactions involving halogen atoms between 5,11,17,23-tetrabromo-25,26,27,28-tetrabutoxy thiacalix[4]-arene (**1**) molecules comprising hetero-macrocyclic host compounds in the crystalline state.[6] Interestingly, the crystal structure of **1** indicated that infinite open-network structures consisting of **1** are formed by triangular Br_3 synthon-type halogen–halogen contacts. Further, the accumulation of infinite open-network structures leads to supramolecular assembly formation via complementary intermolecular CH···Br, S–π, and CH–π interactions.

A survey of halogenated thiacalixarene and calixarene derivatives in the Cambridge Structural Database (CSD, v 5.34, 2013) revealed 52 single-crystal structures containing C–X bonds (where X is fluorine, bromine, and iodine; with 44 C–Br and 8 C–I species (including 1 C–F). From these crystal structures, we identified 26 entries with X···X or X···heteroatom distances that were shorter than sum of the respective van der Waals radii between solely host molecules of thia- or calixarenes (including both X···X and X···heteroatom shorter distances in 3 single-crystal structures of them). In fact, halogen bonding and halogen-halogen interactions are rare in supramolecular assemblies in which solely calixarenes and thiacalixarenes are desired,[6] and especially so in the case of intermolecular interactions between macrocyclic compounds involving halogen atoms. Our interest is focused on the use of hetero-macrocyclic organoiodide species such as iodo–modified thiacalix[4]arene derivatives based on the following criteria: (1) elemental iodine has the strongest polarizing power of the halogen atoms, and; (2) elemental sulfur atoms at linking positions in the thiacalixarene skeleton are ideal electron donors for supramolecular assembly. Thus, macrocyclic iodo-thiacalix[4]arene molecules would likely possess stronger halogen atom–based intermolecular interactions compared to that of **1**, owing to an increasing polarization in the order Cl < Br < I; strongly polarized $I^{\delta+}$ and $I^{\delta-}$ moieties of neighboring macrocyclic organoiodides would potentially act as donors and acceptors for halogen-halogen interactions or halogen bonding, depending on the nature of atom polarization. The aim of this work is to elucidate the nature of halogen bonding and halogen–halogen interactions between iodo-thiacalix[4]arene derivatives in the crystalline state, in comparison with that of **1**. In addition, as our interest also extends to the exploration of halogen bonding involving elemental sulfur, we decided to investigate rare S···I interactions in the thiacalixarene molecules based on relevant reports demonstrating S···I halogen bonding contacts.[7]

Herein, we demonstrate the formation of two supramolecular assemblies constructed via preferential intermolecular halogen–halogen interaction and halogen bonding motifs; these novel assemblies are based on 5,11,17,23-tetraiodo-25,26,27,28-tetrapropoxythiacalix[4]arene (**2**) and 5,11,17,23-tetraiodo-25,26,27,28-tetrabutoxythiacalix[4]arene (**3**) macromolecules (Scheme 1). The elucidation of halogen–halogen interaction and halogen bonding between the macrocyclic host molecules from both crystallographic and computational perspectives provides further support for hydrogen bonding, S–π interactions, and CH···I interactions in both crystalline states.

Results and discussion

Thiacalixarenes **2** and **3** were synthesized as follows: treatment of 5,11,17,23-tetrabromo-25,26,27,28-tetrapropoxy thiacalix-[4]arene or 5,11,17,23-tetrabromo-25,26,27,28-tetrabutoxy thiacalix[4]arene with *tert*-butyllithium in THF at –78°C under nitrogen, followed by addition of I_2, afforded the crude brown products of **2** or **3**. The resulting solids were allowed to recrystallize from ethyl acetate; colorless crystals of pure **2** and **3** were obtained and characterized by single-crystal X-ray diffraction studies and other appropriate methods.

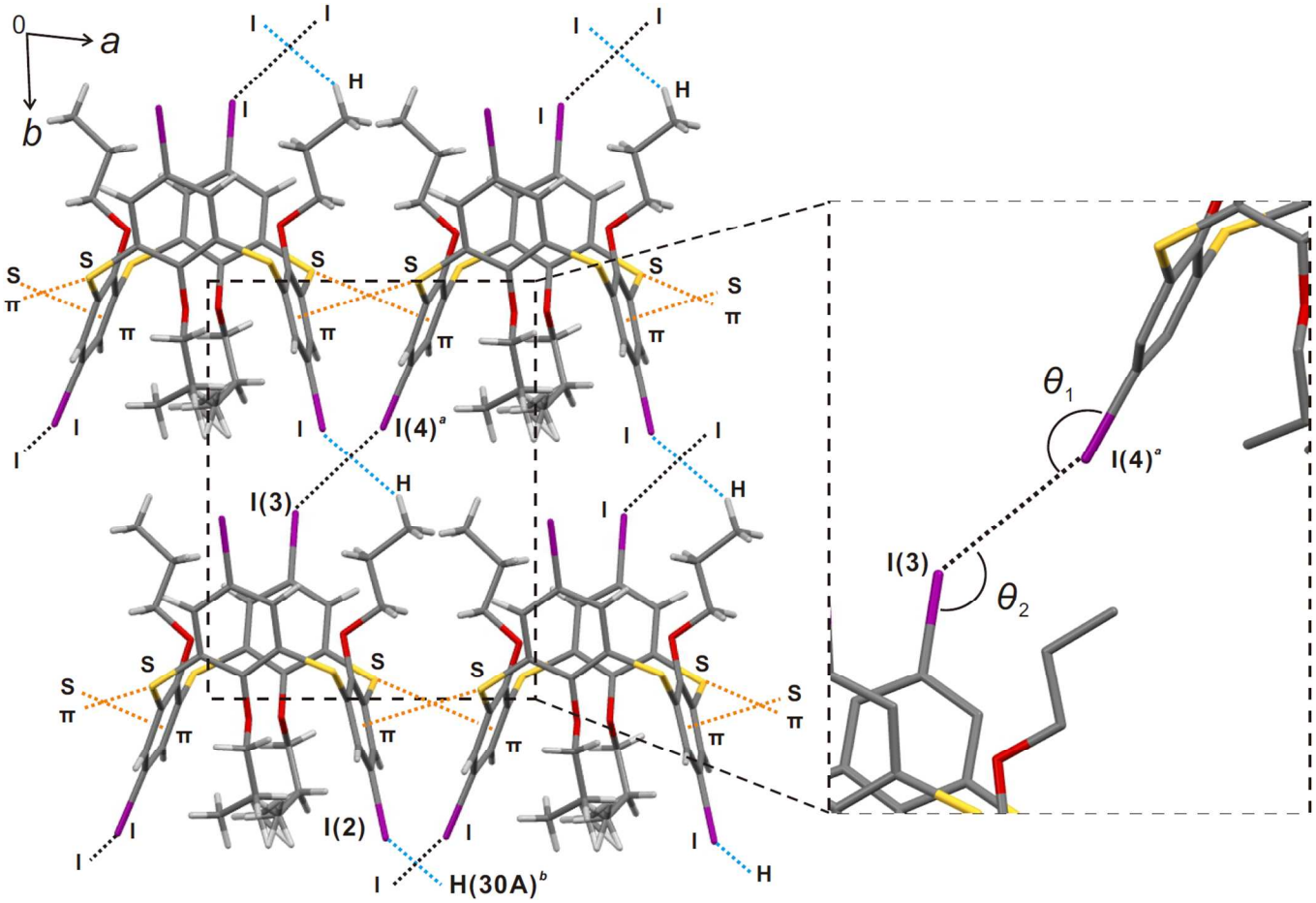

Fig. 2 Stick diagram showing I···I interactions (black dotted lines), CH···I interactions (light-blue dotted lines), and S–π interactions (orange dotted lines) in the crystal structure of **2**, viewed along the [110] plane. The enlarged figure shows the distance and angles of the I···I contact. Symmetry operations: [a], 1+*x*, –1+*y*, *z*; [b], *x*, 1+*y*, *z*.

Single crystals of **2** suitable for single-crystal X-ray diffraction studies were obtained from ethyl acetate over the course of one week. The guest-free crystals of **2** were obtained as colorless platelets which crystallized in the triclinic space group *P*–1, in which one thiacalixarene molecule comprises the asymmetric unit; within this unit, a molecule of **2** exists as the 1,3-alternate conformer, which includes one disordered propyl group appended to the C aromatic ring (Fig. 1). The molecule **2** did not incorporate ethyl acetate as a guest molecule into the cavity. Within the molecular structure of **2**, the adjacent A, B, and C aromatic rings are flipped slightly inward (angles for I(1)–O(1)–O(3), I(2)–O(2)–O(4), and I(3)–O(3)–O(1) angles are 104.71(5)º, 100.50(5)º, and 101.79(5)º, respectively), whereas the D aromatic ring is flipped slightly outward (the I(4)–O(4)–O(2) angle is 113.84(5)º) (ESI; Fig. S2). As mentioned above, thiacalixarene **2** functions as a building block in the formation of a three-dimensional supramolecular network assembly via complementary intermolecular interactions. Accordingly, the crystal structure of **2** suggested that the outward D aromatic ring and the inward C aromatic ring orientations would have a significant influence on increased opportunities for I···I interactions. Additionally, the inward-oriented A and B aromatic rings indicate the likelihood of intermolecular C–H···S hydrogen bonding and C–H···I interactions between molecules of **2**.

Symmetry expansion of the crystal structure of **2** revealed the existence of an I···I interaction between each of the thiacalixarene molecules along the [110] plane (Fig. 2). The crystals of **2** observed here exhibit a halogen–halogen interaction corresponding to Type II, indicated by the ellipsoid shape of the anisotropic iodine atoms of **2** (ESI; Fig. S3). Thus, this interaction of **2** could be described as an attractive electrophile–nucleophile Type II contact. As observed in the crystal structure of **2**, the individual C or D iodo groups of each thiacalixarene molecule induce formation of an I···I interaction between each neighboring thiacalixarene molecule. The θ_1 and θ_2 angles are 155.4(1)º and 129.4(1)º, respectively. The I(3)···I(4)^a interhalogen distance is 3.8805(3) Å, ca. 2% shorter than sum of the van der Waals radii of two iodine atoms (Σ = 1.98 + 1.98 = 3.96 Å). This result suggests that the observed halogen–halogen interaction between the thiacalixarene molecules was weaker in comparison with previous reports.[3] This weakening of the I···I interaction can be attributed to the significant steric bulk of **2** inhibiting contact with the adjacent thiacalixarene molecules. However, comparison with the results of our recent research shows that the I···I distance is shorter

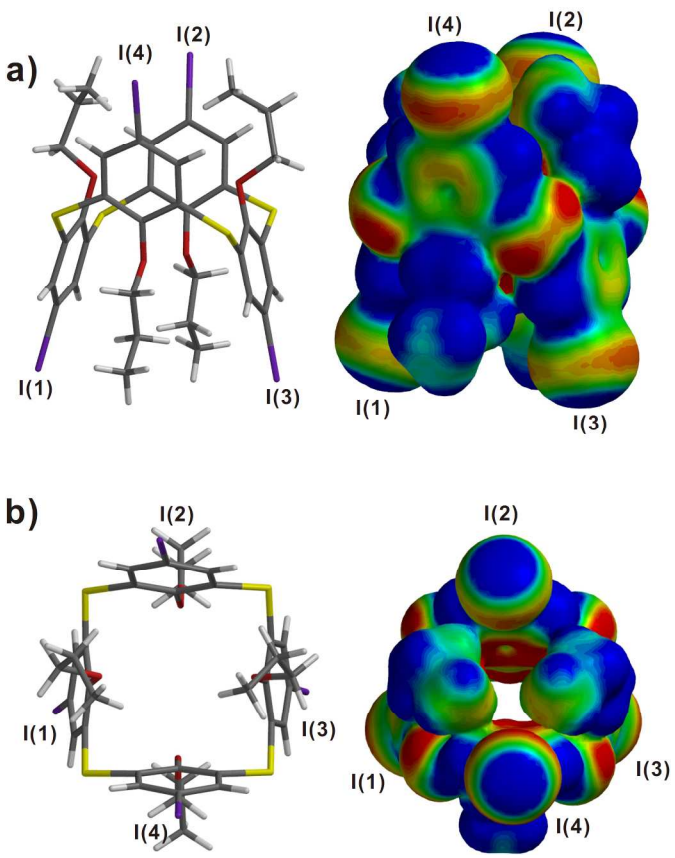

Fig. 3 *Ab initio* electrostatic potential surface of the molecular unit of **2**. a) Stick diagram (left) and electrostatic potential surface (right) showing the side view of the molecular unit of **2**. b) Top view of the molecular unit of **2**. The molecular unit of **2** is shown looking into the iodine atoms to compare the induced negative (red), neutral (green), and positive (blue) electrostatic potentials around the iodine atoms. The potential energies are presented only in the –50.0000 to +50.0000 kJ/mol range to emphasize the variation in electrostatic potential associated with the iodine atoms. The calculated electrostatic potential surface indicates the polarized positive regions (blue) at end caps along the C-I bonds and negative rings (from red to yellow) on the iodine atoms. In the two left-hand diagrams, I = purple, S = yellow, O = red, C = gray, H = white.

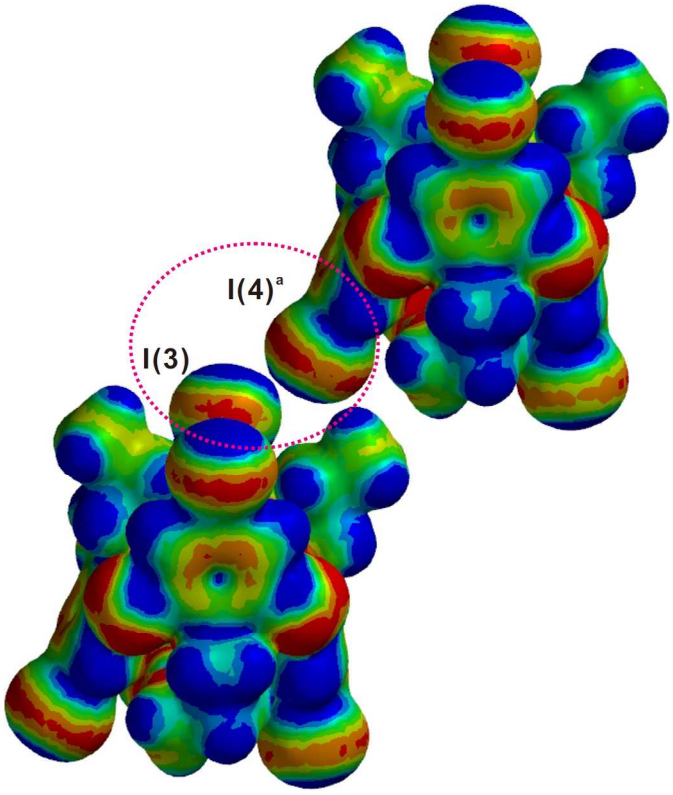

Fig. 4 *Ab initio* electrostatic potential surface of two molecular units of **2**. The potential energies are presented in the –20.0000 to +50.0000 kJ/mol range. The electrostatic potential surface indicates that the Type II $I^{\delta+}\cdots I^{\delta-}$ interaction occurs between the polarized regions consisting of positive end caps (blue) along the aromatic C-I bonds and negative rings (from red to yellow) perpendicular to them on the iodine atoms. Symmetry operations: [a], 1+*x*, –1+*y*, *z*.

than the Br···Br distances in the observed in crystals of **1** (Br···Br distances are 3.6603(6) and 3.6994(6) Å in addition to ca. 1.1% and 0.01% shorter than sum of van der Waals radii of two bromine atoms in the crystals of **1** (Σ = 1.85 + 1.85 = 3.70 Å).[6] Through this comparison with **1**, it can be interpreted that macrocycle **2** possesses stronger $I^{\delta+}\cdots I^{\delta-}$ interaction than the $Br^{\delta+}\cdots Br^{\delta-}$ interactions of **1** owing to increased polarization of the iodo group. Additionally, the X···X shorter distances between the macrocyclic thia- and calixarene derivatives revealed 18 single-crystal structures as the result of CSD survey. When comparing the single-crystal structures of CSD survey with that of **2**, seven single-crystal structures of them might be classified as Type II halogen–halogen interactions, which are similar to X···X interaction in crystals of **2**. However, extended structure of **2** did not fit similar patterns in CSD survey. Further examination of the three-dimensional supramolecular assembly of **2** revealed the presence of C–H···I and S–π interactions when viewed along the [110] plane. The C–H···I interactions exist between the iodo group of arene B of the base thiacalixarene molecule and the hydrogen atom of methyl group B belonging to the nearest adjacent thiacalixarene molecule (the C(30)[b]–H(30A)[b]···I(2) distance is 3.1697(3) Å). The observed S–π interactions are displayed between arenes B and D of the base thiacalixarene and the bridging sulfur atoms of the neighboring thiacalixarene molecules in the crystals. These interactions are categorized as Type I because the divalent sulfur atoms are located at the centers of the aromatic rings (ESI; Fig. S4).[8] The *r* distance from the divalent S(1) to the nearest aromatic ring center of arene B (C(7)[c]–C(12)[c]) is 3.746 Å, and the *d* distance from the S(1) atom to the nearest ring-edge carbon atom of arene B (between C(11)[c] and C(12)[c]) is 3.613 Å. In addition, the angles of C(5)–S(1)–arene B centroid and C(23)–S(1)–arene B centroid are 98.22º (α) and 155.24º (α'), respectively. The S(1)–arene B centroid–edge carbon atom φ angle is 74.36º. Conversely, the *r* distance from S(3)[c] to the nearest aromatic ring centroid (arene D, C(19)–C(24)) is 3.782 Å, and the *d* distance from the S(3)[c] atom to the nearest ring-edge carbon atom of arene D (C(23)–C(24)) is 3.636 Å. The angles between C(11)[c]–S(3)[c]–arene D centroid and C(17)[c]–S(3)[c]–arene D centroid are 96.77º (α) and 159.60º (α'), respectively. The S(3)[c]–centroid–edge carbon atom φ angle is 73.85º. Additionally, when viewed along the [011] plane, aromatic C–H···S hydrogen bonding is also observed in the crystal structure of **2**. Hydrogen bonding (H···S) between the

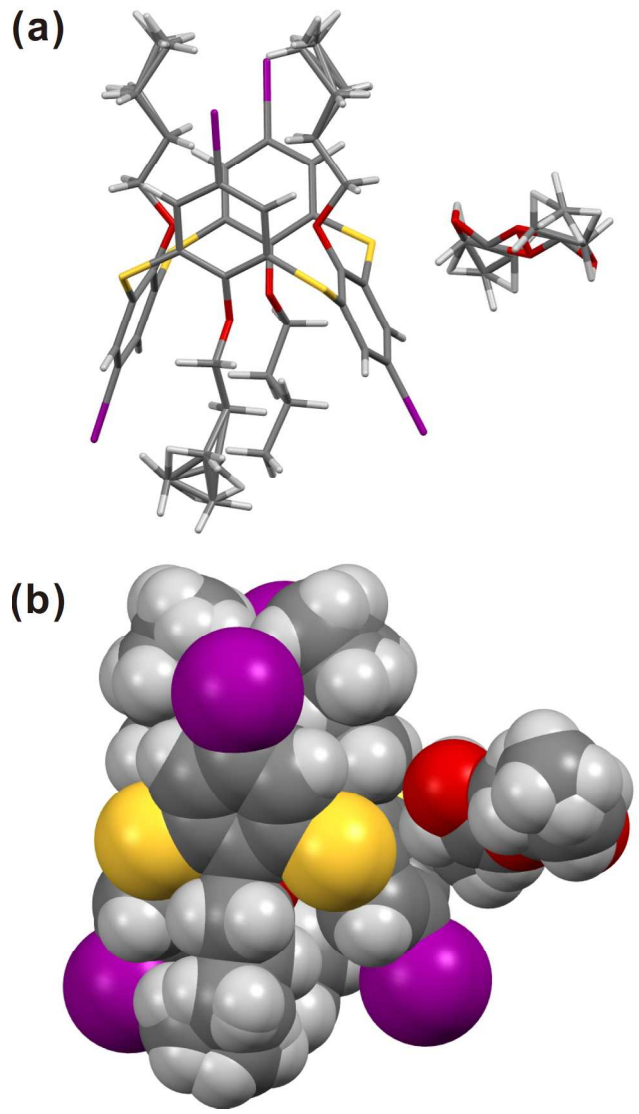

Fig. 5 (a) Stick diagram and (b) space-filling representation of the molecular structure of **3** and ethyl acetate as a guest molecule. I = purple, S = yellow, O = red, C = dark grey, H = light gray.

hydrogen atoms of arenes A and C of the base thiacalixarene and the linking sulfur atoms of S(2)^{d} and S(4)^{e} of the neighboring thiacalixarenes are observed (the H(2)···S(2)^{d} and H(14)···S(4)^{e} distances are 2.7619(7) and 2.9413(8) Å, respectively) (ESI; Fig. S5). Thus, the three-dimensional supramolecular assembly of **2** constructed from preferential intermolecular I···I halogen–halogen interactions and aromatic–H···S hydrogen bonding is demonstrated and further supported by complementary non-covalent intermolecular contacts of C–H···I and S–π interactions.

To further elucidate the observed halogen-halogen interaction, we employed a computational approach to investigate the halogen-halogen interactions of **2**. The electrostatic potential surfaces of the molecular unit and two intermolecular units in **2** were calculated using DFT methods (EDF2/6-31G(*) level) in Spartan 10^{TM} from the X-ray structure of **2**.[9,10] The calculated electrostatic potential surfaces indicated electron-rich and electron-deficient regions on the iodine atoms of **2**. In the asymmetric unit, an electronic state with polarized $I^{\delta+}$ (blue) and $I^{\delta-}$ (red) regions at different angles on the iodine atoms was clearly observed (Fig. 3). In addition, the electrostatic potential surface shows that the ring-like surfaces lie perpendicular to the direction of the aromatic C–I bonds. Correspondingly, the electrostatic potential surface indicates that the polarized regions consist of positive end caps along the aromatic C-I bonds and negative rings perpendicular to them on the iodine atoms. This result suggests that the approximate angles of the polarized iodine atoms of the molecule play a dominant role in the assembly of two intermolecular units via an $I^{\delta+}\cdots I^{\delta-}$ interaction that is categorized as a Type II halogen-halogen interaction in this system (Fig. 4); i.e., in order for two intermolecular $I^{\delta+}\cdots I^{\delta-}$ interactions to form, there must be a close encounter between the electron donor and acceptor, i.e., between the polarized $I^{\delta+}$ region on the iodine atom in one molecule and the polarized $I^{\delta-}$ region on the iodine atom of an adjacent molecule. As discussed above, within the two intermolecular units in the crystals of **2**, the crystal structure suggests that the base and nearest adjacent thiacalixarene molecules are attached through the $I^{\delta+}\cdots I^{\delta-}$ interaction that requires close proximity of the electron-rich and electron-deficient regions on the different iodine atoms.

For macrocycle **3**, single crystals suitable for single-crystal X-ray diffraction studies were obtained from ethyl acetate over a period of one week. Crystals of **3** were obtained as colorless blocks which crystallized in the $P2_1/c$ space group. The asymmetric unit is composed of one thiacalixarene molecule and a half of ethyl acetate molecule as a solvent molecule. However, the guest molecule is not incorporated into the cavity of **3**. Within this unit, the molecular structure of **3** is similar to that of **2**, adopting a 1,3-alternate conformation, which includes three disordered butyl groups appended to the A, C, and D aromatic rings (Fig. 5). The anisotropic iodine atoms of **3** show ellipsoid shapes depending on the nature of halogen atom (ESI; Fig. S6). In the molecular structure of **3**, the oppositely oriented A and C aromatic rings are flipped slightly outward (angles for I(1)–O(1)–O(3) and I(3)–O(3)–O(1) are 115.27(6)º and 111.77(6)º, respectively), whereas the B and D aromatic rings are flipped slightly inward (angles for I(2)–O(2)–O(4) and I(4)–O(4)–O(2) are 104.77(5)º and 107.76(5)º, respectively) (ESI; Fig. S7). The outwardly pointing iodine atom of arene A (having the largest I(1)–O(1)–O(3) angle) permits facile intermolecular S···I halogen bonding between molecules of **3**, whereas the iodine atom of the inward-pointing arene B (having the smaller I(2)–O(2)–O(4) angle) participates in O···I halogen bonding with a disordered ethyl acetate guest molecule.

Additionally, C–H···I and S–π interactions, as well as H···S hydrogen bonding motifs are also observed between the thiacalixarene molecules. In contrast to the crystal structure of **2**, the symmetry expansion of **3** indicates that the iodo group of arene A in the base molecule interacts with the linking sulfur atom of the nearest adjacent thiacalixarene molecule. The I(1)···S(2)^{f} distance and the C(1)–I(1)–S(2)^{f} angle are

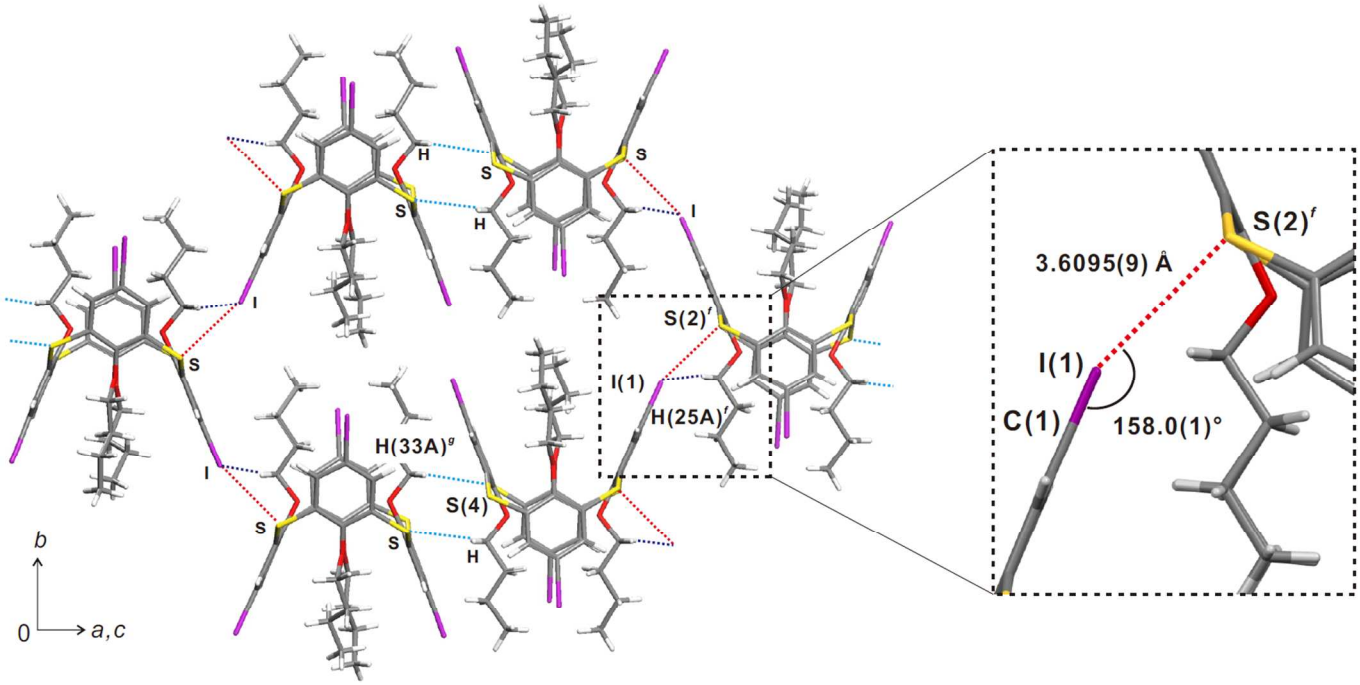

Fig. 6 Stick diagram showing S···I halogen bonding (red dotted lines), CH–I interactions (dark blue dotted lines), and hydrogen bonding (light-blue dotted lines) in the crystal structure of **3**. Disordered moieties have been removed for clarity. The enlarged figure shows the distance and angle of the S···I contact. Symmetry operations: ^{f}; 2–*x*, –1/2+*y*, 3/2–*z*; ^{g}; 1–*x*, 2–*y*, 1–*z*.

3.6095(9) Å and 158.0(1)°, respectively (Fig. 6). The distance is ca. 4.5% shorter than sum of the respective van der Waals atomic radii. Furthermore, the S···I halogen bonding between the macrocyclic thia- and calixarenes has not been found though CSD. In fact, crystals of **3** represent new S···I pattern in the thiacalixarene and calixarene chemistries. When viewed in the same plane, intermolecular C–H···I interactions and butyl moieties C–H···S hydrogen bonding are also observed. A C–H···I bonding interaction between the iodo group of arene A in the base thiacalixarene and the hydrogen atom of a neighboring thiacalixarene butyl group is noted (the C–H(25A)^f···I(1) distance is 3.1138(3) Å). A C–H···S hydrogen bonding motif exists between the bridging sulfur atom of the base thiacalixarene molecule and the butyl hydrogen atom of arene C in the neighboring thiacalixarene (the C–H(33A)^g···S(4) distance is 2.9953(9) Å). A Type II S–π interaction is observed in the crystal structure of **3**, categorized as such because the divalent sulfur atom of the neighboring thiacalixarene makes contact on the edges of arene B of an adjacent molecule (ESI; Fig. S8).[8] When comparing the S–π interaction of **2** with that of **3**, only one contact is made to the nearest adjacent thiacalixarene; although crystals of **2** exhibit continuous S–π interactions with respect to each other along the [110] plane, the crystals of **3** lack this continuity between neighboring thiacalixarene molecules. The distance from the divalent S(2)^h to the nearest aromatic ring center (*r*) is 3.928 Å, and the distance from the S(2)^h to the nearest ring-edge carbon atom between C(7) and C(8) (*d*) is 3.514 Å. In addition, the two angles of the C(3)^h–S(2)^h–arene B centroid (C(7)–C(12)) and the C(9)^h–S(2)^h–arene B centroid are 96.27° (*α*) and 154.49° (*α′*), respectively, and the S(2)^h–arene B centroid–edge carbon atom (between C(7) and C(8)) angle is 61.36° (*φ*) (ESI; Fig. S9). Interestingly, O···I halogen bonding is also observed between the iodine atom of arene B and the oxygen atom of a disordered ethyl acetate (ESI; Fig. S10). The O(5)^i···I(2) distance and angle are 2.932(7) Å and 176.3(2)°, respectively, indicating that this halogen bonding motif is stronger than the aforementioned S···I contact, i.e., ca. 15.7% shorter than the sum of van der Waals radii of oxygen and iodine atoms. When viewed along the [101] plane, a C–H···I interaction is observed between the iodo group of aromatic ring A in the base thiacalixarene molecule and a hydrogen atom of butyl group B in the nearest neighboring thiacalixarene molecule (the measured C–H(29B)^j···I(1) distance is 3.1568(3) Å; ESI, Fig. S11). Although the crystal structures of **2** and **3** adopt the same conformers, two different, weak, non-covalent intermolecular interactions of halogen atoms (halogen-halogen interaction and halogen bonding) are observed in the extended structures of **2** and **3**. As the results of crystallographic analysis of **2** and **3** demonstrate, the iodine atom of **3** (compared to that of **2**) displays preferential S···I halogen bonding because the longer alkyl chain of **3** prevents I···I interaction due to the steric hindrance around the iodine atoms of **3**. This may therefore suggest that the iodine atom of **3** is able to interact with the thiacalixarene sulfide group and ethyl acetate as a solvent molecule via halogen bonding.

Crystallographic analysis of **3** revealed that two halogen bonding contacts are observed with respect to each macrocyclic molecule or between the macrocyclic molecules and the guest molecules. The supramolecular architecture of **3** is thus formed

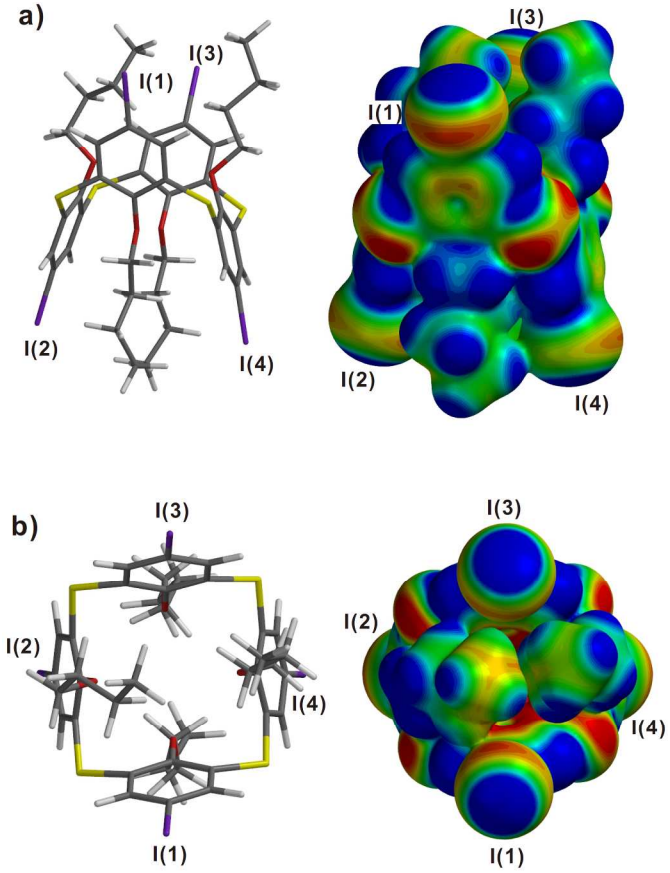

Fig. 7 *Ab initio* electrostatic potential surface of the molecular unit of **3**. a) Stick diagram (left) and electrostatic potential surface (right) showing side view of the molecular unit of **3**. b) Top view of the molecular unit of **3**. The molecular unit of **3** is shown looking into the iodine atoms to compare the induced negative (red), neutral (green), and positive (blue) electrostatic potentials around the iodine atoms. The potential energies are presented only in the –50.0000 to +50.0000 kJ/mol range to emphasize the variation in electrostatic potential associated with the iodine atoms. The calculated electrostatic potential surface indicates the polarized positive regions (blue) at end caps along the C-I bonds and negative rings (from red to yellow) on the iodine atoms. The calculated electrostatic potential surface also shows polarizable iodine atoms as electrophilic species at end caps (electron acceptors, blue) and the linking sulfur as lone pairs–possessing species (electron donors, red). In the two left-hand diagrams, I = purple, S = yellow, O = red, C = gray, H = white.

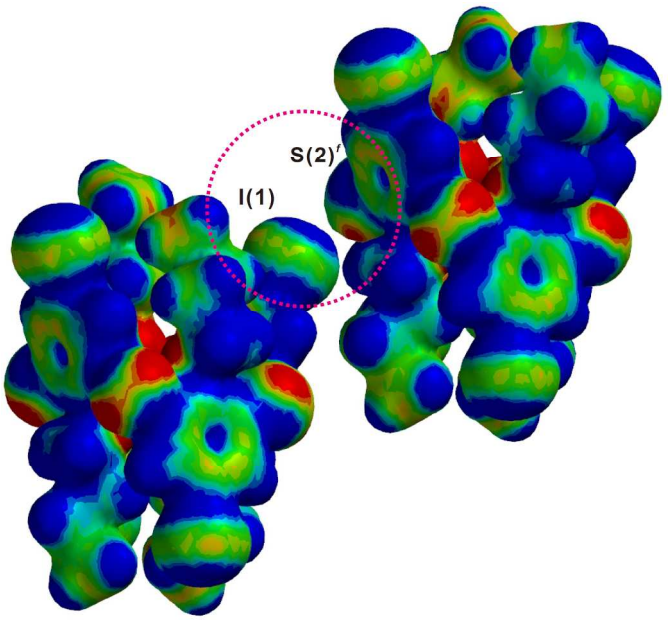

Fig. 8 *Ab initio* electrostatic potential surface of the two molecular units of **3**. The potential energies are presented in the –10.0000 to +110.0000 kJ/mol range. The electrostatic potential surface shows that the S···I halogen bonding occurs between the positive end caps (blue) on the iodine atom (I(1)) and the negative lone pair (red) on the sulfur atom (S2)^{f}. Symmetry operations: ^{f}; 2–*x*, –1/2+*y*, 3/2–*z*.

via assembly though preferred S···I and H···S bonding contacts; furthermore, supramolecular assembly through complementary non-covalent intermolecular contacts of C–H···I, I···O halogen bonding, and S–π interactions is observed.

In order to rationalize the observed S···I halogen bonding, we also employed a computational approach to further elucidate the S···I halogen bonding of **3**. The electrostatic potential surfaces of the regions at different angles on the iodine atoms were also observed (Fig. 7). In addition, the electrostatic potential surface indicates that the polarized regions consist of positive end caps along the aromatic C-I bonds and negative rings perpendicular to them on the iodine atoms (in the same manner as **2**), and the bridging sulfur atoms have negative regions depending on their lone pairs. The results of the computational investigation showed polarizable iodine atoms as electrophilic species along the aromatic C–I bonds at the end caps (electron acceptors) and the linking sulfur as lone pair–possessing species (electron donors) in Lewis acid–base pairs, suggesting that the angle of the polarized iodine atoms and the lone pairs of the bridging sulfide groups of each molecule play an important role in the establishment of the two intermolecular units via a S···I interaction in this system (Fig. 8). Accordingly, in order for two intermolecular S···I interactions to form, it is necessary for a close encounter between the electron donor and acceptor to occur, i.e., between the polarized I positive region (blue) on the iodine atom in one molecule and the S negative region (red) on the lone pairs of the sulfur atom of the nearest molecule. As discussed above, within the two intermolecular units in the crystals of **3**, the crystal structure of **3** suggests that the base and nearest adjacent thiacalixarene molecules are attached through S···I halogen bonding that requires close proximity of the electron donors and electron acceptors in Lewis acid–base pairs.

Conclusions

We have demonstrated the presence of intermolecular interactions involving halogen atoms through the crystallographic observations and the computational approaches of iodo-modified thiacalix[4]arene derivatives **2** and **3**; based on the interactions of two different alkyl chains appended to the iodo-substituted thiacalixarene core, two types of halogen–halogen interactions and halogen bonding motifs between the macrocycles were structurally observed. Two very distinct types of halogen-based intermolecular interactions could be observed to exist between the thiacalixarene skeletons in the

macrocyclic assembly: (1) short I···I halogen–halogen interactions in **2** (ca. 2% shorter than the respective van der Waals radii), and; (2) short S···I halogen bonding in **3** (ca. 4.5%). These two observations can be correlated to the presence of the linking sulfur heteroatoms of the thiacalixarene molecules, which are thus noted to have a profoundly significant effect on supramolecular assembly; these contributions to halogen-based intermolecular interactions are rare in solely macrocyclic compounds. Crystallographic studies of intermolecular interactions as valuable design elements are also of biological and engineering importance, especially in the interaction of thyroid hormones with proteins[4f] and the fabrication of functional organic materials such as porous solids[4d]. We are currently exploring the synthesis of iodinated thiacalix[4]arenes with different alkyl chains, as well as investigating the possibility that supramolecular assemblies can be formed from new thiacalixarene molecules in the crystalline state through halogen bonding or halogen-halogen interactions.

Acknowledgements

We thank Dr. Hiroshi Katagiri (Graduate School of Science and Engineering, Yamagata University, JP) and Mr. Noritaka Uchida (Wavefunction, Inc. Japan Branch Office) for their valuable discussions and technical support on the single-crystal X-ray diffraction studies and the quantum chemical calculations.

Experimental

All reactions were carried out under a nitrogen atmosphere. Tetrahydrofuran (THF) was distilled from sodium/benzophenone under nitrogen and stored over activated 4 Å molecular sieves. 5,11,17,23-Tetrabromo-25,26,27,28-propoxythiacalix[4]arene[11] and 5,11,17,23-tetrabromo-25,26,27,28-butoxythiacalix[4]arene[6] were prepared by the bromination and alkylation of the upper and lower rims, respectively, of 25,26,27,28-hydroxythiacalix[4]arene, followed by recrystallization from a 1:1 cyclohexane/chloroform mixture, according to published procedures. ^{1}H and ^{13}C NMR spectra were recorded in $CDCl_3$ on a JEOL 600SSS ECA-600 instrument. Chemical shifts are quoted as parts per million (ppm) relative to tetramethylsilane. Infrared (IR) spectra were recorded on a Thermo Fisher Scientific Nicolet iS5 spectrophotometer. Elemental analysis was performed using a Systems Engineering CE-440M CHN/O/S elemental analyzer.

Synthesis of 5,11,17,23-tetraiodo-25,26,27,28-tetrapropoxy thiacalix[4]arene (2)

tert-Butyllithium (2.49 mL of a 1.65 M solution) was slowly added to a solution of 5,11,17,23-tetrabromo-25,26,27,28-propoxythiacalix[4]arene (0.5 g, 0.510 mmol) in THF (28 mL) at –78ºC. The reaction mixture was stirred for 20 min, and a solution of I_2 (1.42 g, 5.61 mmol) in THF (2.5 mL) was added at –78ºC. The dark-brown solution was stirred for 3 h at room temperature. The reaction mixture was poured into aqueous NH_4Cl (100 mL) and extracted with chloroform (2×50 mL). The organic phase was washed with saturated aqueous $Na_2S_2O_3$ (2×50 mL), and saturated aqueous $NaHCO_3$ (2×50 mL), and dried over anhydrous Na_2SO_4. The solvent was evaporated under reduced pressure to yield the crude product as a brown solid. Recrystallization from ethyl acetate yielded **2** as colorless crystalline blocks (0.14 g, 23.4%). IR (ATR) ν cm^{-1}: 3049, 2961, 2873, 1542, 1419, 1236, 1087, 1059, 867, 734; ^{1}H NMR ($CDCl_3$): δ 7.68 ppm (s, 8H, Ar-*H*), 3.88 (t, 8H, O-C*H*$_2$-), 1.34 (m, 8H, -C*H*$_2$-), 0.78 (t, 12H, -C*H*$_3$); ^{13}C NMR ($CDCl_3$): δ 159.8, 140.6, 130.4, 85.4, 71.3, 22.7, 10.2 ppm. Calcd. for $C_{36}H_{36}I_4O_4S_4$: C, 37.00; H, 3.10. Found: C, 37.20; H, 2.90.

Synthesis of 5,11,17,23-tetraiodo-25,26,27,28-tetrabutoxy thiacalix[4]arene (3)

The procedure for the synthesis of **3** was followed, using *tert*-butyllithium (2.49 mL of a 1.65 M solution), 5,11,17,23-tetrabromo-25,26,27,28-butoxythiacalix[4]arene (0.5 g, 0.482 mmol) and I_2 (1.35 g, 5.30 mmol), yielding the desired compound as colorless crystalline blocks (0.26 g, 44.1%). IR (ATR) ν cm^{-1}: 3044, 2954, 2869, 1539, 1422, 1236, 1088, 1061, 867, 758. ^{1}H NMR ($CDCl_3$): δ 7.67 ppm (s, 8H, Ar-*H*), 3.91 (t, 8H, O-C*H*$_2$-), 1.21 (m, 16H, -C*H*$_2$-), 0.99 (t, 12H, -C*H*$_3$); ^{13}C NMR ($CDCl_3$): δ 159.5, 140.0, 130.4, 85.5, 69.4, 31.6, 19.3, 14.7 ppm. Calcd. for $C_{36}H_{36}I_4O_4S_4$·$EtOAc_{0.5}$: C, 39.50; H, 3.80. Found: C, 39.80; H, 3.50.

X-Ray crystallography

Single crystals of **2** and **3** suitable for X-ray diffraction studies were grown from ethyl acetate by slow evaporation at room temperature. The crystals were extracted from, the mother liquor with a glass pipette, and placed in paraffin oil. The single crystals coated with oil were isolated on MicroMounts™, and immediately placed in a cold nitrogen stream at 100 K. X-Ray diffraction data for **2** and **3** were collected on a Rigaku PAXIS RAPID imaging plate diffractometer equipped with graphite-monochromated Mo-Kα radiation (λ = 0.71075 Å). The structures were solved by direct methods using SHELXS-97,[12] and refined using the full-matrix least-squares method on F^2 using SHELXL-97.[13]

Crystal data for 2: $C_{36}H_{36}I_4O_4S_4$, *Fw* = 1168.54, crystal dimensions = 0.30 × 0.30 × 0.20 mm, colorless, triclinic, space group *P*–1, *a* = 9.9688(5), *b* = 12.4158(6), *c* = 17.4099(10) Å, α = 86.1612(15), β = 79.7348(18), γ = 80.1653(15)º, *V* = 2087.70(19) Å^3, *Z* = 2, ρ_{calcd} = 1.859 g cm^{-3}, μ = 3.221 mm^{-1}, *F*(000) = 1120.00, and $2\theta_{max}$ = 27.51º. A total of 20628 reflections were collected, of which 9457 reflections were independent (R_{int} = 0.0319). Two propyl groups showed disorder at two positions (A and B sites), which were refined anisotropically. The parts containing C(33A) and C(33B) were refined as the disordered propyl moiety, the occupancies of which were fixed at 0.79 and 0.21, respectively. The structure was refined to a final *R* = 0.0287 for 8018 data points [$I > 2\sigma(I)$] with 437 parameters, with *wR* = 0.0788 for all data, GOF = 1.097, and a residual electron density max/min = 1.420/–

1.270 e Å^{-3}. The residual electron densities are associated with iodine atoms, mainly one peak of 1.42 which reside around 0.9 Å of I(3). The supplementary crystallographic data for this paper can be found in CCDC entry 946918; the data can be obtained free of charge from the Cambridge Crystallographic Data Centre via www.ccdc.cam.ac.uk/data_request/cif.

Crystal data for 3: $C_{42}H_{48}I_4O_5S_4$, *Fw* = 1268.70, crystal dimensions = 0.25 × 0.20 × 0.20 mm, colorless, monoclinic, space group $P2_1/c$, a = 18.4313(9), b = 14.2656(5), c = 17.8550(6) Å, β = 92.4043(10)º, V = 4690.5(4) Å^3, Z = 4, ρ_{calcd} = 1.796 g cm^{-3}, μ = 2.877 mm^{-1}, $F(000)$ = 2464.00, and $2\theta_{max}$ = 27.48º. A total of 44777 reflections were collected, of which 10723 reflections were independent (R_{int} = 0.0488). Three butyl groups showed disorder at two positions (A and B sites), which were refined anisotropically. The parts containing C(27A)/C(28A) and C(27B)/C(28B) were refined as the disordered butyl moiety, the occupancies of which were fixed at 0.5532 and 0.4468, respectively. The parts containing C(35A)/C(36A) and C(35B)/C(36B) were refined as the disordered butyl moiety, the occupancies of which were fixed at 0.5105 and 0.4895, respectively. The parts containing C(39A)/C(40A) and C(39B)/C(40B) were refined as the disordered butyl moiety, the occupancies of which were fixed at 0.8011 and 0.1989, respectively. One ethyl acetate solvent molecule also showed disorder, which was refined anisotropically. The occupancy was fixed at 0.5. The structure was refined to a final R = 0.0351 for 8700 data points [$I > 2\sigma(I)$] with 526 parameters, with wR = 0.0860 for all data, GOF = 1.036, and a residual electron density max/min = 1.860/–1.550 e Å^{-3}. The residual electron density is associated with iodine atoms, mainly one peak of 1.86 which reside around 0.8 Å of I(3). The supplementary crystallographic data for this paper can be found in CCDC entry 946919; the data can be obtained free of charge from the Cambridge Crystallographic Data Centre via www.ccdc.cam.ac.uk/data_request/cif.

Atomic numbering of crystal structures of 2 and 3

The crystal structure of 2: the carbon atoms in the phenyl rings are C(1)–C(24), and the carbon atoms of the *n*-propyl groups are C(25)–C(36), where C(1)–C(6) = ring A, C(7)–C(12) = ring B, C(13)–C(18) = ring C, and C(19)–C(24) = ring D, in line with the schematic formula of **2** as shown in Scheme 1. The oxygen atoms O(1)–O(4) are appended at C(4), C(10), C(16), and C(22), the sulfur atoms S(1)–S(4) at C(3), C(5), C(9), C(11), C(15), C(17), C(21), and C(23), and the iodine atoms I(1)–I(4) at C(1), C(7), C(13), and C(19).

The crystal structure of 3: the carbon atoms in the phenyl rings are C(1)–C(24), and the carbon atoms of the *n*-butyl groups are C(25)–C(40), where C(1)–C(6) = ring A, C(7)–C(12) = ring B, C(13)–C(18) = ring C, and C(19)–C(24) = ring D, in line with the schematic formula of **3** as shown in Scheme 1. The oxygen atoms O(1)–O(4) are appended at C(4), C(10), C(16), and C(22), the sulfur atoms S(1)–S(4) at C(3), C(5), C(9), C(11), C(15), C(17), C(21), and C(23), and the iodine atoms I(1)–I(4) at C(1), C(7), C(13), and C(19). The carbon and oxygen atoms of the co-crystallized ethyl acetate molecule are C(41)–C(44) and O(5)–O(6), respectively.

Theoretical calculations for 2 and 3

Spartan 10^{TM} software was used for the single-point energy calculations of the X-ray structures of **2** and **3**.[10] The disordered moieties in **2** and **3** (propyl groups in **2**, butyl groups in **3**) were omitted from the calculations based on the X-ray structures of **2** and **3**. Because the H-C bonds are short in the X-ray structures of **2** and **3**, only the heavier atoms were frozen; the molecular structures and two-molecule structures of **2** and **3** were then minimized, whereupon the positions of the hydrogen atoms were then relaxed. Single-point energy calculations were carried out as density functional theory (DFT) calculations at the EDF2 level using the *ab initio* 6-31G (*) basis set.

Notes and references

[a] Center for Geo-Environmental Science (CGES), Graduate School of Engineering and Resource Science, Akita University, 1-1 Tegatagakuen-machi, Akita 010-8502, Japan. E-mail: myamada@gipc.akita-u.ac.jp; Fax: +81 18 889 3068; Tel: +81 18 889 3068
[b] Department of Life Science, Faculty of Engineering and Resource Science, Akita University, 1-1 Tegatagakuen-machi, Akita 010-8502, Japan.
[c] Department of Applied Chemistry for Environments, Graduate School of Engineering and Resource Science, Akita University, 1-1 Tegatagakuen-machi, Akita 010-8502, Japan. E-mail: hamada@gipc.akita-u.ac.jp; Fax: +81 18 889 2440; Tel: +81 18 889 2440

† Electronic Supplementary Information (ESI) available: Supplementary figures, crystallographic data for **2** and **3**, and CCDC entries 946918 and 946919 (in CIF format). See DOI: 10.1039/b000000x/

1 (a) J. –M. Lehn, *Supramolecular Chemistry: Concepts and Perspectives*; Wiley-VCH: Weinheim, Germany, 1995; (b) J. W. Steed, D. R. Turner and K. J. Wallace, *Core Concepts in Supramolecular Chemistry and Nanochemistry*; John Wiley & Sons Ltd: West Sussex, England, 2007; (c) Organic Nanostructures; J. L. Atwood and J. W. Steed, Eds.; Wiley-VCH: Weinheim, Germany, 2008; (d) D. N. Reinhoudt and M. Crego-Calama, *Science*, 2002, **295**, 2403–2407.

2 (a) F. Meyer and P. Dubois, *CrystEngComm*, 2013, **15**, 3058–3071; (b) M. Erdélyi, *Chem. Soc. Rev.*, 2012, **41**, 3547–3557; (c) D. Hauchecorne, A. Moiana, B. J. van der Veken and W. A. Herrebout, *Phys. Chem. Chem. Phys.*, 2011, **13**, 10204–10213; (d) V. R. Hathwar, R. G. Gonnade, P. Munshi, M. M. Bhadbhade and T. N. G. Row, *Cryst. Growth Des.*, 2011, **11**, 1855–1862; (e) A. C. Legon, *Phys. Chem. Chem. Phys.*, 2010, **12**, 7736–7747; (f) Metrangolo, P.; Resnati, G. *Science*, 2008, **321**, 918–919; (g) P. Metrangolo, F. Meyer, T. Pilati, G. Resnati and G. Terraneo, *Angew. Chem., Int. Ed.*, 2008, **47**, 6114–6127.

3 (a) R. B. K. Siram, D. P. Karothu, T. N. G. Row and S. Patil, *Cryst. Growth Des.*, 2013, **13**, 1045–1049; (b) M. B. Andrews and C. L. Cahill, *Dalton Trans.*, 2012, **41**, 3911–3914; (c) T. T. T. Bui, S. Dahaoui, C. Lecomte, G. R. Desiraju and E. Espinosa, *Angew. Chem., Int. Ed.*, 2009, **48**, 3838–3841; (d) F. F. Awwadi, R. D. Willett, K. A. Peterson and B. Twamley, *Chem. Eur. J.*, 2006, **12**, 8952–8960; (e) B. K. Saha, R. K. R. Jetti, L. S. Reddy, S. Aitipamula and A. Nangia, *Cryst. Growth Des.* 2005, **5**, 887–899; (f) V. R. Pedireddi, D. S. Reddy, B. S. Goud, D. C. Craig, A. D. Rae and G. R. Desiraju, *J. Chem. Soc., Perkin Trans. 2*, 1994, 2353–2360.

4 (a) T. Kida, T. Iwamoto, H. Asahara, T. Hinoue and M. Akashi, *J. Am. Chem. Soc*., 2013, **135**, 3371–3374; (b) K. Raatikainen and K. Rissanen, *Chem. Sci*., 2012, **3**, 1235–1239; (c) T. Ogoshi, *J. Inclusion Phenom. Macrocyclic Chem*., 2012, **72**, 247–262; (d) A. R. Voth, F. A. Hays and P. S. Ho, *Proc. Natl. Acad. Sci. USA*, 2007, **104**, 6188–6193; (e) M. V. Rekharsky, H. Yamamura, M. Kawai, I. Osaka, R. Arakawa, A. Sato, Y. H. Ko, N. Selvapalam, K. Kim and Y. Inoue, *Org. Lett*. 2006, **8**, 815–818; (f) P. Auffinger, F. A. Hays, E. Westhof and P. S. Ho, *Proc. Natl. Acad. Sci. USA*, 2004, **101**, 16789–16794.

5 (a) Jentzsch, A. V.; Emery, D.; Mareda, J.; Nayak, A. K.; Metrangolo, P.; Resnati, G.; Sakai, N.; Matile, S. *Nat. Commun.* 2012, **3**, 1–8. (b) Parisini, E.; Metrangolo, P.; Pilati, T.; Resnati, G.; Terraneo, G. *Chem. Soc. Rev*., 2011, **40**, 2267–2278. (c) Metrangolo, P.; Carcenac, Y.; Lahtinen, M.; Pilati, T.; Rissanen, K.; Vij, A.; Resnati, G. *Science*, 2009, **323**, 1461–1464. (d) Metrangolo, P.; Neukirch, H.; Pilati, T.; Resnati, G. *Acc. Chem. Res*., 2005, **38**, 386–395.

6 M. Yamada, Y. Ootashiro, Y. Kondo and F. Hamada, *Tetrahedron Lett*., 2013, **54**, 1510–1514.

7 (a) H. D. Arman, R. L. Gieseking, T. W. Hanks and W. T. Pennington, *Chem. Commun*., 2010, **46**, 1854–1856; (b) D. Cinčić, T. Friščič and W. Jones, *Chem. Eur. J*., 2008, **14**, 747–753; (c) T. Imakubo, T. Shirahata, M. Kibune and H. Yoshino, *Eur. J. Inorg. Chem*., 2007, 4727–4735; (d) J. I. Jay, C. W. Padgett, R. D. B. Walsh, T. W. Hanks and W. T. Pennington, *Cryst. Growth Des*., 2001, **1**, 501–507.

8 C. –Q. Wan, J. Han and C. W. M. Thomas, *New J. Chem*., 2009, **33**, 707–712

9 (a) P. J. Stephens, F. J. Devlin, C. F. Chabalowski and M. J. Frisch, *J. Phys. Chem*., 1994, **98**, 11623–11627; (b) G. Rauhut and P. Pulay, *J. Phys. Chem*., 1995, **99**, 3093–3100; (c) G. Rauhut and P. Pulay, *J. Am. Chem. Soc*., 1995, **117**, 4167–4172.

10 Spartan 10™, Wavefunction Inc., Irvine, CA, USA, 2010.

11 Hamada, M. Yamada, Y. Kondo, S. Ito and U. Akiba, *CrystEngComm*, 2011, **13**, 6920–6922.

12 G. M. Sheldrick, *SHELXS-97: Program for Solution of Crystal Structures*, University of Göttingen, Germany, 1997.

13 G. M. Sheldrick, *SHELXL-97: Program for Refinement of Crystal Structures*, University of Göttingen, Germany, 1997.

Graphic Abstract

Halogen–halogen interaction and halogen bonding in thiacalixarene systems

Manabu Yamada*[,a], Ryo Kanazawa[b], and Fumio Hamada*[,c]

[a] Center for Geo-Environmental Science (CGES), Graduate School of Engineering and Resource Science, Akita University, 1-1 Tegatagakuen-machi, Akita 010-8502, Japan

[b] Department of Life Science, Faculty of Engineering and Resource Science, Akita University, 1-1 Tegatagakuen-machi, Akita 010-8502, Japan

[c] Department of Applied Chemistry for Environments, Graduate School of Engineering and Resource Science, Akita University, 1-1 Tegatagakuen-machi, Akita 010-8502, Japan

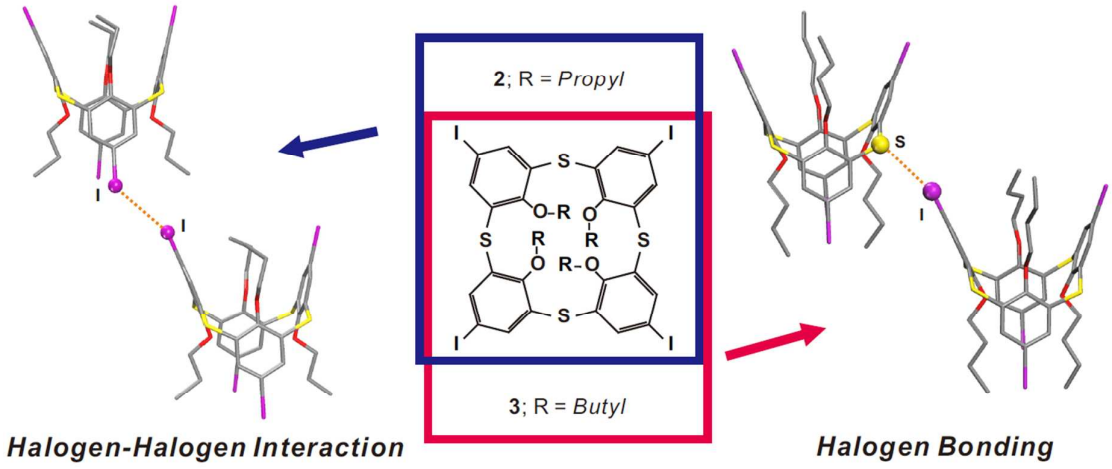

Crystals of 5,11,17,23-tetraiodo-25,26,27,28-tetrapropoxythiacalix[4]arene (**2**) exhibited I···I halogen–halogen interaction between each of the thiacalixarene molecules, ca. 2% shorter than the respective van der Waals atomic radii. In contrast, crystals of 5,11,17,23-tetraiodo-25,26,27,28-tetrabutoxy thiacalix[4]arene (**3**) was identified to have S···I halogen bonding ca. 4.5% shorter than the respective van der Waals atomic radii. We have also elucidated I···I and S···I interactions by computational approaches (see picture; I = purple, S = yellow, O = red, and C = gray).